Data Evaluation of Bone Development

Aichun Chen
Diana Lubyanaya

Advisor: Dr. Joyce Keyak

Department of Radiological Sciences
University of California, Irvine

August 18, 2012

Abstract

The concept of bone density has shown to be essential in the understanding of bone development and the identification of pediatric diseases. Starting from the eary 1990s, several methods have been developed to obtain the bone denstiy for pediatric study, but no specific approach was absorbed to measure the accurate volumetric bone density. Our research efficiently utilizes the newly developed tomography technique to obtain the bone density. A sufficient amount of bone density values will be calculated to set a density range for pediatrics. We believe that this density range generated from the Computed Tomography technique will increase our understanding of pediatric bone fractures and bone development.

1 Introduction

In order to identify pediatirc diseases and fully understand the development of a normal bone, we have considered bone density to be the key factor in our research. Many children, especially boys, are exposed to a high percentage of bone fratures [2]. Many people suspect that it may be due to the lack of necessary nutrition or, in other cases, obesity.[2, 6, 10] However, research has shown two basic causes for increased rates of bone fractures in children. The first is based on the decreasing volumetric bone mineral density (vBMD) during the rapid pubertal development, and the second is the lag between areal bone mineral density (aBMD) and the increase in body weight. To enhance our understanding of complex factors contributing to pediatric diseases, we developed a technique to quantify bone density.

Currently, there is no one specific approach to find the volumetric bone density. Even though there exists a few different methods to measure bone density, such as dual energy X-ray absorptionmetry (DXA) and the Quantititative Untrasound (QUS), they unfortunately share excessive deficits in giving accurate bone density measurements. Instead, we utilized the CT scanner technique to generate a 3-Dimensional image of the human body. This technique allowed us to visualize the entire bone structure. Then we developed a computer program to convert the brightness of the image into Hounsfield units and, ultimately, determine the bone density. From the bone density and volume, we were able to calcualte the bone mass. Because of the advantage of generating a 3-Dimensional image, we measured the bone size and geometric properties of the bone to acquire an accurate volumetric bone density. Overall, we have applied a developed method to calculate the bone denstiy of the vertebral bodies. The resulting data will help us understand the detection and treatment of

pediatric diseases.

2 Research Focus

2.1 Why the spinal vertebrae?

The human body experiences dramatic changes in its skeletal structure in its progression from an infancy stage (of over 300 bones) to a full grown adult stage (of only 206 bones) over the course of its lifetime. Because in this process the body changes in mass and structure, the greatest change of the human body is absorbed by the spine. The spine's unique curved shape contributes to free movements, balance check, and shock absorption. These qualities enriched our curiousity to study the pediadric spine and lead us to the focus of our study.

The spine consists of three main regions: cervical, thoracic, and lumbar areas. The cervical region (C1-C7) is the upper fraction of the spine, and it functions to provide the neck movement and weight bearing of the head. Next is the thoracic region (T1-T12) that is located at the center of the spine. It is the area attached to the rib cage in order to protect the inner organs. This detail will later help us determine the location of different vertebrae. Lastly is the lumbar region (L1-L5). Its vertebrae are significantly greater in volume, thus its shape and size allow it to fulfill its primary purpose of bearing the human body weight [5]. Intuitively, the two lower regions of the spine may exhibit the largest changes in bone development; thus, the functions of the thoracic and lumbar areas in the human body influenced our further investigation of children's bone development and triggered our urge to understand the change in pediatric bone density.

Each spinal region differentiates into individual vertebraes that hold their own structures and functions. Particularly, our target is focused on each vertebra because they are the building blocks of the spinal complex. Every vertebra is composed of different parts that contribute to the proper movement of the spine. The main components of the vertebra are processes, facets, and the drum-shaped body. We are mainly interested in the drum-shaped body, as it functions to withstand compression and bear the human body weight.

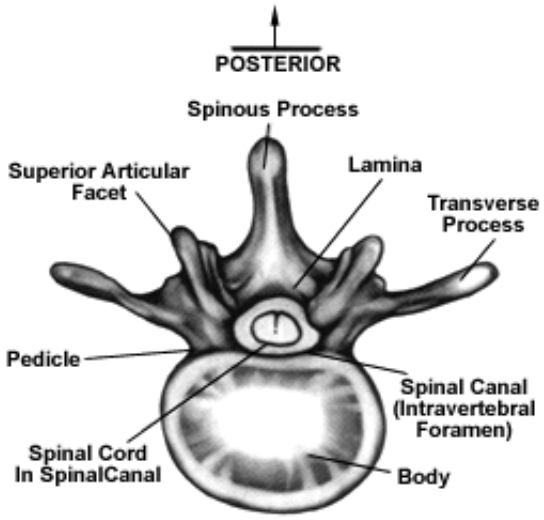

Figure 1: The Vertebra Structure.
This is an example of a normal vertebra [11]

2.2 Using the total bone density

In our research, we have took in account different bone material compositions to define the bone density. It is a challenge to define the definition of bone density because bone is made up of two types of bone tissues - trabecular bone tissue and cortical bone tissue /citeMethods. We have included both tissues in our measurements to avoid the ambiguity of distinguishing the boundary between bone tissues. In general, we attained the the entire periosteum of the bone and set its density based on the the defaults of hydroxylapatite phantom tubes. The density of the hydroxylapatite tubes are given in mg/cc; therefore, the bone density calculated from the linear regression equation is in term of the equivalent mineral bone density.

3 Methods

The methods used to measure bone density have gradually improved over the years. With the de-

velopment of computer technology, one of the first strategies for regional measurements of bone density was introduced in 1980s, known as the dual energy X-ray absorptiometry (DXA) [2]. Since its strategy was to create simply a 2-Dimensional image of the bone structure, the true volumetric bone density was not possible to obtain. However, DXA was remarkably advantageous in calculating the area bone density using the following formula:

$$aBMD = \frac{BoneMieralContent(g)}{BoneArea(cm^2)}$$

In addition to DXA, another tactic was established in the realm of assessing bone density, called the quantitative ultrasound (QUS). The QUS method measures the speed of sound (SOS) and broadband attenuation (BUA) at different peripheral regions. SOS depends not only on bone density but also on bone stiffness. Due to the dramatical change in the cortical bone distribution over a period of time, the SOS can be affected by the thickness of the cortical bone, which will then influence the final QUS results and cause inconsitency in data interpretation. Because of its unreliable output, QUS is inappropriate to use for calculation of the total bone denstiy [2].

The third and final method in bone density technology is known as the peripheral quantitative computed tomography (pQCT), which has recently become popular among bone reseachers in understanding the development of the bone. The greatest advantage of the CT Scanner is the generation of a 3-Dimensional image which enables the assessment of a variety of bone parameters related to bone size and geometirc structure. The pQCT method exposes the use of displayed field of view (DFOV), pixels, and Hounsfield units to allow total bone density calculations, including mass and volume. In our research, we constructed a program that converts the brightness of each voxel in a CT scan to CT numbers. This method produces direct results that would help our further analysis.

4 Procedure

4.1 Locate vertebrae

In order to proceed with our research, we must be able to distinguish the vertebrae in order to locate them. Initially, we searched for clues that would help us identify which region we were looking at. The best way to start the search was to look for the thoracic region which has the rib cage attachment, and then label each vertebrae from T1 to T12. A similar technique was used following T12, except that the rib cage was no longer visible in the lumbar area.

Most of the CT scanners make more than 100 slice images per subject, meaning that each vertebrae may have more than once slice. Therefore, we had to chose the best slice that would reveal the fullest image of each vertebrae. It was our responsibility to avoid ambiguous contrasts in the slices and make careful judgements, where the vertebrae bone would begin and where it would end, to have the most accurate results possible. Accuracy within the contrasts played a major role the contours of the chosen slices.

4.2 Derive contours

Contouring is an important process in deriving and outlining given slices. Because we were able to locate the vertebrae and chose the best slices, we were prepared to proceed to contouring. Since only a fraction of slices were chosen for contouring, about 10 contours were expected from each subject. Adjusting the contrast of the images and using the zooming option in the control panel allowed us to see a detailed view of the pixels to ascertain the location of the contours. A computer was developed to perform a contouring algorithm that distinguishes apart different gray levels of the images. The average threshold for most of the slices was entered as 1200; however, it could be adjusted in accordance to the CT numbers of the slices.. The value of the threshold can be understood by the meaning of CT numbers. The definition of a CT number extracts from a Hounsfield unit (HU) that measures the attenuation of a given material..The scale for a CT number is based on values of 0 for air and 1000 for water. Through thorough evaluation of the outlines, we made sure the pixels were on and inside the

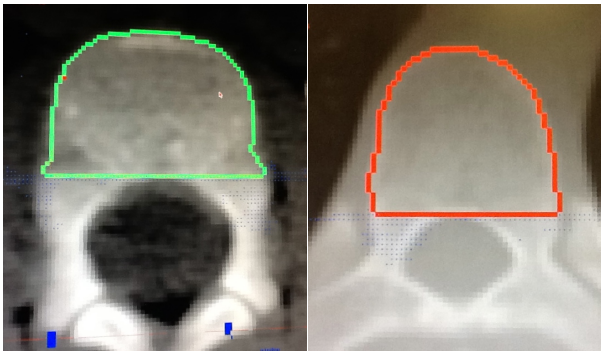

Figure 2: Contours of Different Subject Groups.
The image on the left shows a 17-year-old vertebra, while on the right is the 3-year-old vertebra. The shape of the vertebrae is significantly differ.

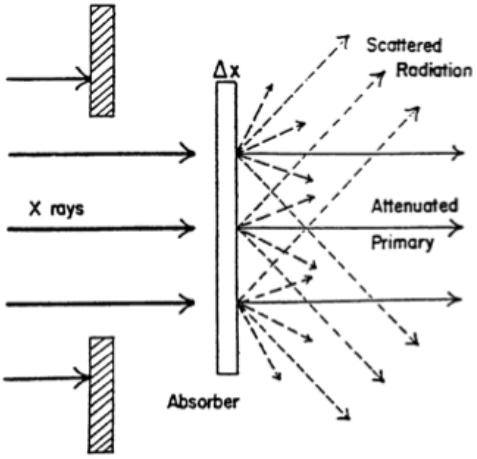

Figure 3: Photon Entry into the Material.
Photon absorption into the delta x provided initial and final intensities with the depth. [4]

contours.

Certain aspects of our procedure had to be customized according to the age of the subject. For example, the vertebrae of a 3-year-old possess a developing phase with incomplete bone configuration. In this case, the vertebrae body was not fully connected. The incomplete structure of the vertebrae body created some difficulties when deriving the contours. In other cases, the threshold needed to be adjusted to include all the necessary pixels on the edges. These small gaps in the drum had to be neglected and noted as still developing tissue, which left some room for a source of error in our data analysis.

The explicit steps of the program sent a "seed" pixel to search from left to right across the row until it would find a starting pixel whose CT numbers were above the threshold value. The first pixel would start the contouring, and the program would examine the succeeding 8 pixels to find the next pixel that meets the threshold value. The process would continue in a counterclockwise direction to define the outline of the vertebrae drum.

When a closed contour of a slice is finally completed, the contour may be modified to get the most perfect desired outline. At the edge of the contour, extra slices would be deleted to include only the pixels with specified gray levels. In addition, all the pixels not located inside the contour would be erased. The contour would be saved in a file in the control panel. This entire process was repeated and done to all of our subjects. These results would help us in our further steps of calibration and data analysis.

4.3 Calibration and data analysis

Calibration leads our research to the final steps of finding the total bone density, volume, and mass. However, it is crucial to first understand the science behind the CT apparatus. The technology of the CT scanner emits a fraction of photons that generate the production of a CT scan. Each photon contributes to the brightness of ranging densities of the bone mineral. Because we are dealing with photons entering a material at certain a depth, we must introduce the importance of the attenuation coefficient (μ). The attenuation coefficient has the following formula

$$I = I_o e^{-\mu x}$$

where I_o represents intial photon intensity, I is the final photon intensity, and x is the depth of the a given material [3]. Knowing this derivation directs us to the next point in determining the Hounsfield unit (HU). The Hounsfield unit is defined as

$$HU = 1000 * [\frac{\mu(E_{CT}) - \mu_w E_{CT}}{(\mu_w E_{CT})}]$$

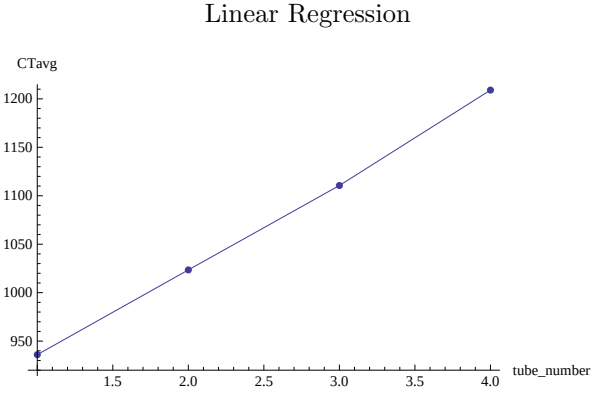

Figure 4: Linear Regression Equation: $y = 90.6101x + 843.25$ Linear regression is plotted on the average CT number vs. the tube number. This is an example of a slice that has been analysed in terms of the linear regression.

with E_{CT} being the effective energy tranmitted by the CT scanner and the subscript w representing water [3]. Having the value of HU, we can proceed to the CT number value. The CT number can be computed simply by adding 1000 to the HU. This CT number approach helps us avoid negative numbers and simplifies our calculations.

Every CT scan slice has three or four embedded tubes at the bottom of the phantom to set the brightness defaults. Using a computer program, we determined the average CT number of each tube and performed a linear regression analysis. This linear regression provided us with a formula that helped us determine the calibration equation, which has the following form:

$$\text{Density (mg/cc HA)} = (\text{slope})(\text{CT}) + \text{intercept}$$

For example, we included the data of one slice belonging to a 3-year-old subject. We took the average CT number of each tube and ploted the CT values on the graph with respect to the tube numbers to have the linear regression shown in Figure 4.

The next step required us to determine the CT numbers of each individual pixel in the contour. After substituting the CT number into the density equation, we were able to determine the density of each individual pixel. The summation of all the pixels produced an average bone density of the entire contour.

ID	Type	# slices	DFOV (cm)	pixel size
1	Abd/Pelvis	160	40.0	0.7813
2	Abd/Pelvis	152	39.9	0.7793
3	Abd/Pelvis	72	31.7	0.6191
4	Abd/Pelvis	45	25.3	0.4941
4	Chest	57	25.9	0.5059

Figure 5: Table of Pixels and Related Data. This is a quick summary of the general values of the four different subjects. Pixel size will be crucial in the calculation of volume.

To determine the value of the volume, we first calculated the pixel size. The pixel size is the field of view (DFOV) per matrix, and the thickness of each CT slice was set to 3mm. From these data sets, we were able to calculate the volume for each slice. Both, density and volume give the mass, therefore, we have reached our goal in developing the calculation method for studying the pediatric bone develpment. Further computation and data analysis may help us make systematic conclusions about the bone density range.

However, this was only a manual calculation and a way to check the computer generated calibration. Up to this point we are in the process of manipulating the computer program to function properly and provide us with precise and quick calculations that would determine the density, volume, and mass of all of our subjects.

5 Conclusion

As a result, we were able to determine the volumetric bone density using the linear regression of the average CT numbers and the values of individual pixel size. With the assistance of the default function of the CT scan, we were able to obtain the necessary data to calculate the bone volume and mass. The methodology of the data analysis has shown the requirement of excessive computing. It would be much more efficient to use a computer to boost the process of data analysis. Our future work focuses on automatic computing for our future data analysis. Meanwhile, the manual calibration serves as a means of comparison and validation of the computer calculations. With

the speed and efficiency of computer calculations, we will be able to analyze data for more vertebrae and slices. We would also like to acquire more subjects from the UCI Medical Center to build a sufficient data set. Those data will later enable us to find a range of bone density among different ages. The final range would utilize those data to help identify pediatric diseases.

References

[1] Manasi Agrawal, Shitij Arora, Jianjun Li, Rabin Rahmani, Li Sun, Adam F. Steinlauf, Jeffrey I. Mechanick, and Mone Zaidi. Bone, inflammation, and inflammatory bowel disease. *Current Osteoporosis Reports*, 9(4):251–257, 2011.

[2] Teresa L. Binkley, Ryan Berry, and Bonny L. Specker. Methods for measurement of pediatric bone, 2008.

[3] Saxby Brown, Dale L. Bailey, Kathy Willowson, and Clive Baldock. Investigation of the relationship between linear attenuation coefficients and ct hounsfield units using radionuclides for spect, 2008.

[4] Carl A Carlsson and Gudrun Alm Carlsson. *Basic Physics of X-ray imaging.* Number LiH-RAD-R-008. Institution for medicine och vard, 2 edition, 1996.

[5] Mayfield Clinic and Spine Institute. Anatomy of the spine. www.mayfieldclinic.com, August 2012.

[6] K.J. Ellis, R.J. Shypailo, W.W. Wong, and S.A. Abrams. Bone mineral mass in overweight and obese children: diminished or enhanced? *Acta Diabetologica*, 40:s274–s277, 2003.

[7] H. Franck and M. Munz. Total body and regional bone mineral densitometry (bmd) and soft tissue measurements: Correlations of bmd parameter to lumbar spine and hip. *Calcified Tissue International*, 67(2):111–115, 2000.

[8] H J Kalkwarf, B S Zemel, V Gilsanz, J M Lappe, M Horlick, S Oberfield, S Mahboubi, B Fan, M M Frederick, K Winer, and J A Shepherd. The bone mineral density in childhood study: bone mineral content and density according to age, sex, and race. *J Clin Endocrinol Metab*, 92(6):2087–2099, Jun 2007.

[9] T S Kaneko, J S Bell, M R Pejcic, J Tehranzadeh, and J H Keyak. Mechanical properties, density and quantitative ct scan data of trabecular bone with and without metastases. *J Biomech*, 37(4):523–530, Apr 2004.

[10] Emilie Rocher, Christine Chappard, Christelle Jaffre, Claude-Laurent Benhamou, and Daniel Courteix. Bone mineral density in prepubertal obese and control children: relation to body weight, lean mass, and fat mass. *Journal of Bone and Mineral Metabolism*, 26(1):73–78, 2008.

[11] P.A. South Texas Spinal Clinic. Anatomy of the spine, 2004-2009.